on Src tyrosine kinase activity (Fig. 3*b*). Crosslinking of small MAG had no appreciable effect on Fyn kinase activity (Fig. 3*c*). We therefore conclude that the crosslinking of large MAG specifically activates Fyn tyrosine kinase. Activation of Fyn kinase was also observed on crosslinking of large MAG using polyclonal anti-MAG antibody obtained from rabbits immunized with purified MAG (Fig. 3*d*). The time courses of tyrosine phosphorylation of Fyn and large MAG after the crosslinking paralleled the change in Fyn kinase activity (Fig. 3*e*).

We showed that the crosslinking of large MAG activates Fyn kinase in cotransfected COS cells. To determine how its activation is reflected in myelinogenesis, we examined large MAG-associated kinase activity during myelination (Fig. 4*A*). Immunoprecipitation of large MAG revealed that the activity of large MAG-associated kinase was highest during the initial stage of myelination (P4) and decreased thereafter (Fig. 4*A*, *a* and *b*), like the kinase activity of total myelin Fyn (Fig. 1*e*). Evaluation of the co-immunoprecipitating kinase by peptide mapping revealed that the large MAG-associated kinase was Fyn (Fig. 4*A*, *c*).

To confirm the interaction of Fyn and large MAG *in vivo*, we examined the localization of Fyn and large MAG during brain development (Fig. 4*B*). By using $+/fyn^{Z}$ heterozygous mice, in which the unique region of the *fyn* gene on one of the alleles was fused to the bacterial *lacZ* gene in-frame, expression of Fyn was followed by LacZ expression[18]. Large MAG expression was monitored by immunohistochemistry. During the early stage of myelination (P7), Fyn and large MAG showed striking co-localization in fibre tracts and oligodendrocytes (Fig. 4*B*), suggesting their interactions during early myelinogenesis. We then analysed whether homozygous *fyn*-deficient mice could form myelin. Electron microscopic analysis revealed that the *fyn*-deficient mice formed myelin (data not shown), which is consistent with a previous report[19]. However, the amount of myelin per brain (w/w) of *fyn*-deficient mice was about 50–60% of that of age-matched wild-type mice (Fig. 4*C*, *a*). In addition, immunoblotting of brain lysates with antibodies specific for neuron (neuron-specific enolase) and myelin (myelin basic protein) revealed that 50% less myelin was present in *fyn*-deficient mice than in wild-type mice, whereas there was virtually no difference in the amount of neuron between wild-type and *fyn*-deficient mice (Fig. 4*C*, *b*). These findings indicate that myelination is partially impaired in *fyn*-deficient mice. Moreover, we detected large MAG-associated kinase in *fyn*-deficient mice, which might compensate for Fyn function (Fig. 4*C*, *c*). The kinase may belong to the Src family, and was active during the early stages of myelination, as is Fyn kinase in normal mice (Fig. 4*A*, *a*, *C*, *c*). The kinase activity was much weaker than that of normal mice, which would explain the inefficient myelination.

We propose that the interaction of large MAG with its ligand on neuronal axons generates a biological signal that involves the rapid activation of Fyn at the beginning of myelination. This signalling may be an important part of myelinogenesis. □

Received 7 June; accepted 31 December 1993.

1. Duncan, I. D., Skoff, R. P. & Colman, D. (eds) *Myelination and Dysmyelination* (New York Academy of Sciences, New York, 1990).
2. Lemke, G. *Neuron* **1,** 535–543 (1988).
3. Norton, W. T. & Podusio, S. E. *J. Neurochem.*, **21,** 749–757 (1973).
4. Umemori, H. *et al. Molec. Brain Res.* **16,** 303–310 (1992).
5. Cooper, J. A. in *Peptides and Protein Phosphorylation* (ed. Kemp, B.) 85–113 (CRC Press, Boca Raton, 1990).
6. Salzer, J. L., Holmes, W. P. & Colman, D. R. *J. Cell Biol.* **104,** 957–965 (1987).
7. Sternberger, N. H., Quarles, R. H., Itoyama, Y. & Webster, H. de F. *Proc. natn. Acad. Sci. U.S.A.* **76,** 1510–1514 (1979).
8. Johnson, P. W. *et al. Neuron* **3,** 377–385 (1989).
9. Poltrak, M. *et al. J. Cell Biol.* **105,** 1893–1899 (1987).
10. Edwards, A. M. *et al. Molec. cell. Biol.* **8,** 2655–2658 (1988).
11. Veillette, A., Bookman, M. A., Horak, E. M. & Bolen, J. B. *Cell* **55,** 301–308 (1988).
12. Samelson, L. E., Phillips, A. F., Luong, E. T. & Klausner, R. D. *Proc. natn. Acad. Sci. U.S.A.* **87,** 4358–4362 (1990).
13. Yamanashi, Y., Kakiuchi, T., Mizuguchi, J., Yamamoto, T. & Toyoshima, K. *Science* **251,** 192–194 (1991).
14. Eiseman, E. & Bolen, J. B. *Nature* **355,** 78–80 (1992).
15. Hatakeyama, M. *et al. Science* **252,** 1523–1528 (1991).
16. Sudol, M., Grant, S. G. N. & Maisonpierre, P. C. *Neurochem. Inc.* **22,** 369–384 (1993).
17. Koch, C. A., Anderson, D., Moran, M. F., Ellis, C. & Pawson, T. *Science* **252,** 668–674 (1991).
18. Yagi, T. *et al. Nature* **366,** 742–745 (1993).
19. Grant, S. G. N. *et al. Science* **258,** 1903–1910 (1992).
20. Yamanashi, Y. *et al. Proc. natn. Acad. Sci. U.S.A.* **89,** 1118–1122 (1992).
21. Okada, M., Nada, S., Yamanashi, Y., Yamamoto, T. & Nakagawa, H. *J. biol. Chem.* **266,** 24249–24252 (1991).
22. Fujita, N. *et al. J. Neurochem.* **55,** 1056–1059 (1990).
23. Sukegawa, J. *et al. Oncogene* **5,** 611–614 (1990).
24. Parsons, S. J., McCarley, D. J., Raymond, V. W. & Parsons, J. T. *J. Virol.* **59,** 755–758 (1986).
25. Fujita, N. *et al. Biochem. biophys. Res. Commun.* **165,** 1162–1169 (1989).
26. Semba, K. *et al. Proc natn. Acad. Sci. U.S.A.* **83,** 5459–5463 (1986).
27. Tanaka, A. *et al. Molec. cell. Biol.* **7,** 1978–1983 (1987).
28. Takebe, Y. *et al. Molec. cell. Biol.* **8,** 466–472 (1988).
29. Turner, J. M. *et al. Cell* **60,** 755–765 (1990).
30. Kunkel, T. A. *Proc. natn. Acad. Sci. U.S.A.* **82,** 488–492 (1985).

ACKNOWLEDGEMENTS. We thank M. Sudol for critical reading of the manuscript; Y. Kadowaki and Y. Yamanashi for discussion; J. Fujimoto, E. Suzuki and K. Hirosawa for microscopic analyses; Y. Shigetani for histochemical analyses; Y. Fukui for GD11; A. Tanaka for *src* cDNA; M. Takeuchi for construction of the Fyn mutants; and N. Fusaki and S. Nagasawa for care of mice.

Glioblastoma growth inhibited *in vivo* by a dominant-negative Flk-1 mutant

Birgit Millauer*, Laura K. Shawver†, Karl H. Plate‡, Werner Risau‡ & Axel Ullrich*§

* Department of Molecular Biology, Max-Planck-Institut für Biochemie, Am Klopferspitz 18A, 82152 Martinsried, Germany
† SUGEN Inc., 515 Galveston Drive, Redwood City, California 94063, USA
‡ Department of Molecular Cell Biology, Max-Planck-Institut für physiologische und klinische Forschung, W. G. Kerckhoff Institut, 61231 Bad Nauheim, Germany

ANGIOGENESIS, the sprouting of capillaries from pre-existing blood vessels, is a fundamental process in the formation of the vascular system during embryonic development. In adulthood, angiogenesis takes place during corpus luteum formation and in pathological conditions such as wound healing, diabetic retinopathy, and tumorigenesis. Vascularization is essential for solid tumour growth and is thought to be regulated by tumour cell-produced factors, which have a chemotactic and mitogenic effect on endothelial cells[1–4]. Vascular endothelial growth factor (VEGF), a homodimeric glycoprotein of relative molecular mass 45,000, is the only mitogen, however, that specifically acts on endothelial cells, and it may be a major regulator of tumour angiogenesis *in vivo*[5,6]. Its expression has been shown to be upregulated by hypoxia, and its cell-surface receptor, Flk-1, is exclusively expressed in endothelial cells[7,8]. Here we investigate the biological relevance of the VEGF/Flk-1 receptor/ligand system for angiogenesis using a retrovirus encoding a dominant-negative mutant of the Flk-1/VEGF receptor to infect endothelial target cells *in vivo*, and find that tumour growth is prevented in nude mice. Our results emphasize the central role of the Flk-1/VEGF system in angiogenesis in general and in the development of solid tumours in particular.

We recently reported the endothelial cell-specific expression of Flk-1 during the development of the mouse vascular system and its function as a receptor for VEGF[7]. To investigate the relevance of Flk-1 as a regulator of endothelial cell growth and angiogenesis, we used a solid-tumour growth model and a dominant-negative strategy that allows interference with receptor tyrosine kinase-mediated signal transduction by formation of inactive dimers after introduction of a signalling-defective receptor mutant into the target cell[9–12]. For delivery of this genetic information, we used replication-defective recombinant retroviruses, which were based on elements of the mouse sarcoma virus (MSV) genome and encoded the complete wild-type Flk-

§ To whom all correspondence should be addressed.

1/VEGF-R (LX Flk-1) or the dominant-negative mutant LX Flk-1 TM under the transcriptional control of the MSV 3′ long terminal repeat (LTR)[13]. The Flk-1 TM mutant lacked 561 C-terminal amino acids of the intracellular kinase domain, but retained transmembrane domain sequences and 23 residues of the cytoplasmic portion of the receptor. As a control, we used a virus mediating the expression of an analogously mutated form of the colony-stimulating factor-1 receptor/c-*fms*.

The capability of Flk-1 TM to form signalling-incompetent heterodimers with the 180K wild-type Flk-1 was demonstrated by coprecipitation of the truncated 130K receptor mutant with an antibody against the C terminus of the intact receptor from lysates of COS cells transiently expressing both forms. As the antibody could not recognize Flk-1 TM, coprecipitation was a result of heterodimerization (Fig. 1*a*). The dominant-negative potential of Flk-1 TM was first examined by measuring its influence on the mitogenic response of Flk-1-expressing NIH3T3 cells after superinfection with the Flk-1 TM virus. As shown in Fig. 1*b*, [^{3}H]thymidine incorporation in the 3T3 Flk-1 cell line was maximally stimulated by 500 pM VEGF, with a half-maximal effective concentration (EC_{50}) of ~100 pM. After superinfection with the Flk-1 TM virus, the Flk-1/VEGF-mediated mitogenic response was dramatically suppressed, even at a ligand concentration of 5 nM. Although 3T3 Flk-1/Flk-1 TM cells expressed wild-type Flk-1 at levels equal to the parental line, they displayed, owing to overexpression of Flk-1 TM, a 6-fold increase of cell-surface receptors, as determined by ^{125}I-labelled VEGF binding (not shown). These results were extended by Flk-1 TM virus-induced suppression of Flk-1 transforming activity (not shown) and showed not only that mutant and wild-type Flk-1 physically associated, but also that this interaction generated signalling-incompetent heterodimers. The dominant-negative inhibitory effect that was achieved at a fivefold excess of Flk-1 TM could not be overcome by a 50-fold ligand excess relative to the EC_{50} value for mitogenic activation. Moreover, Flk-1 TM did not interfere with the signal transduction of the α- and β-PDGF receptors, demonstrating the specificity of its dominant-negative action (data not shown).

To investigate whether Flk-1 function is essential for promotion of tumour angiogenesis, we used C6 rat glioblastoma cells, which produce aggressive subcutaneous tumours in nude mice. *In vitro*, C6 cells secrete VEGF, which is further induced by hypoxia[6,8]. *In vivo*, intracerebral and subcutaneous transplants of C6 cells into syngeneic rats led to upregulation of VEGF messenger RNA in palisading glioblastoma cells surrounding necroses and an increase of Flk-1/VEGF receptor levels in tumour endothelial cells[8], characteristics that make this model indistinguishable from human glioblastoma. Available data suggest that tumour-produced VEGF exerts its chemotactic, mitogenic and possibly differentiation-inducing activities on endothelial cells through the interaction with Flk-1, which results eventually in the establishment of a vascular system in the growing tumour. In case of such a prevalent and crucial role, dominant-negative inhibition of Flk-1 function in endothelial cells surrounding the emerging tumour should prevent its vascularization and consequently suppress tumour growth and disease progression.

To test this model, C6 glioblastoma cells were implanted subcutaneously in nude mice, either alone or with different relative amounts of GP+E86 cells producing comparable titres (1×10^6 CFU ml^{-1}) of recombinant retrovirus. Any direct influence of the retroviruses on the growth of the tumour cells was excluded by growing C6 cells in conditioned media of the different retrovirus-producing cell lines, without any effect on their growth behaviour (data not shown). At regular intervals after implantation, the growth of developing tumours was measured. After about three weeks, mice were killed and their tumours resected for pathological and histological examination. A comparison of the growth curves from the different experimental groups is shown in Fig. 2*a*. The group co-implanted with the control virus-producer cell line, NT c-*fms* TM, showed the same growth behaviour as the implant of C6 cells alone. This was also true for a group co-implanted with GP+E86 cells expressing wild-type Flk-1. In contrast, the group inoculated with retrovirus-producing cells inducing the expression of the Flk-1 dominant-negative deletion mutant, LX Flk-1 TM, had tumour growth dramatically inhibited. The effect was dose-dependent, with a maximum achieved when the virus-producing cells were in 20-fold excess over the tumour cells. There was similar inhibition of C6 glioma tumour growth when Flk-1 TM virus particle-

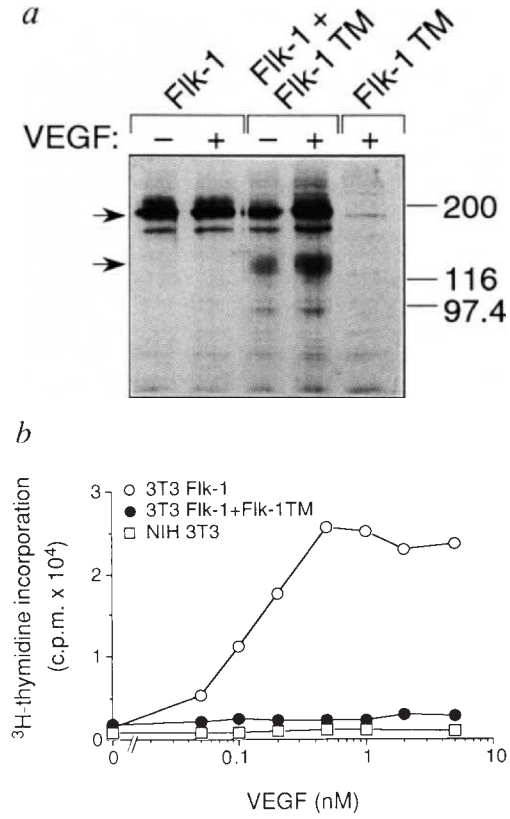

FIG. 1 Dominant-negative inhibition of Flk-1 activity by formation of signalling-defective heterodimers with Flk-1 TM. *a*, COS7 cells were transfected with cytomegalovirus (CMV) promoter-based Flk-1 and Flk-1 TM cDNA expression vectors[17,18]. [^{35}S]methionine-labelled cells were treated with 1 nM VEGF for 3 h at 4 °C, lysed, and analysed by immunoprecipitation with antibody CT128 against the C terminus of Flk-1 (ref. 7) and polyacrylamide gel electrophoresis. *M*, markers are indicated on the right. *b*, VEGF-stimulated [^{3}H]thymidine incorporation of NIH 3T3 cells expressing wild-type Flk-1 alone (3T3 Flk-1) or wild-type Flk-1 and a 5-fold excess of Flk-1 TM (3T3 Flk-1 + Flk-1 TM). Cells were grown to confluence in 12-well dishes (Costar), starved for 2 days in DMEM/0.5% FCS, stimulated with different concentrations of VEGF for 18 h, then incubated with 1 μCi [^{3}H]thymidine per well for 4 h. Incorporation into DNA was determined as described[10].

METHODS. Generation of recombinant retroviruses: The retroviral expression vector pLXSN has been described[13]. LX Flk-1 represents the entire coding region including 5′ and 3′ flanking sequences (4,447 bp) of Flk-1 in pLXSN. LX Flk-1 TM was obtained by ligating the 5′ 2,619 bp of Flk-1 cDNA encoding amino acids 1–806 as a *Cla*I/*Bam*HI fragment to a *Bgl*II/*Hpa*I linker, thereby designing a stop codon 23 amino acids behind the transmembrane region (5′ GTC ATG GAT Ctt cgt taa 3′). In a second step, the *Cla*I/*Hpa*I-fragment was subcloned into the *Cla*I/*Hpa*I site of the pLXSN vector. Stable GP+E86 cell lines producing ecotropic retroviruses expressing the wild-type and mutated receptor constructs were generated as described[10]. Titres were determined by infecting NIH3T3 cells with serial dilutions of virus supernatants followed by G418 selection. Titres of the clones used were ~1×10^6 ml^{-1}. Cell culture: GP+E86 cells were cultured in 225 cm^2 flasks (Nunc) in DMEM/4500 mg l^{-1} glucose (Gibco) supplemented with 10% fetal calf serum.

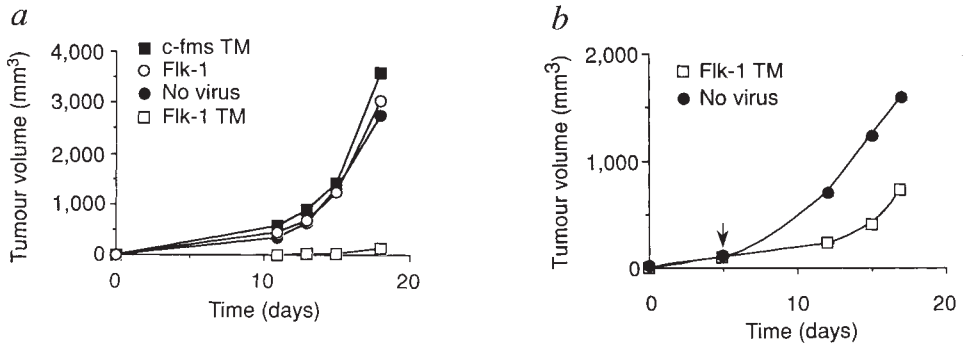

FIG. 2 *a*, Suppression of C6 glioblastoma tumour growth by dominant-negative inhibition of Flk-1. C6 cells (5×10^5) were subcutaneously implanted in nude mice either alone or with 1×10^7 retrovirus-producing cells. Viruses used were LX Flk-1 and LX Flk-1 TM, viruses inducing the expression of wild-type Flk-1 or a dominant-negative Flk-1 mutant under the control of the MLV 3′ LTR, and NT c-*fms* TM, a control virus encoding a dominant-negative c-*fms* mutant analogous in structure to Flk-1 TM under the control of the thymidine kinase promoter. When the first tumours appeared, their volumes were measured every 2–3 days. At the end of the experiment, mice were killed by cervical dislocation and the tumours were resected for pathological and histological examination. The dominant-negative effect was maximal (96%) at 1:20 ratio of C6 tumour cells to virus-producing cells. The inhibition was calculated by comparison of the tumour volumes of the groups co-implanted with LX Flk-1 TM virus-producing cells and control groups. Four animals per group were used, which was confirmed in an independent set of experiments with 8 animals per group. *b*, Inhibition of C6 glioblastoma tumour growth by localized injection of retroviral supernatants. C6 cells (1×10^6) were subcutaneously implanted in nude mice. At day 5 after implantation (arrow), growing tumours were injected with 100 μl retroviral supernatants (corresponding to ~10^5 virus particles) into the site of tumour implantation. Tumour volumes were measured twice a week.
METHODS. Recombinant retroviruses expressing LX Flk-1 and LX Flk-1 TM were determined as for Fig. 1. For generation of NT c-*fms* TM, a stop codon was introduced behind amino acid 541 downstream of the transmembrane region of the c-*fms* cDNA using the oligonucleotide 5′-TTG TAC AAG TAT AAG TAG TAG CCC AGG TAC CAG-3′. The mutated receptor was subcloned in the retroviral expression vector pNTK2 (ref. 19).

containing producer cell supernatants were injected five days after implantation of 10^6 tumour cells, indicating that even established tumours may be suppressed by Flk-1 dominant-negative action (Fig. 2*b*). The transient nature of the effect, however, suggests that for lasting inhibition a continuous supply of high titres of virus is necessary.

To confirm that the inhibition of the C6 glioblastoma growth was caused by dominant-negative action of the retrovirally expressed constructs on endothelial cells, the tumours were resected and analysed. Comparison of whole-mount specimens revealed striking differences: whereas the surface of the control tumours was reddish, as expected for well-vascularized tissue, the inhibited cell implants were very pale (Fig. 3*a*). Histological staining of frozen sections revealed that the control tumours consisted of a homogeneous mass of viable cells (Fig. 3*b*, *d*). Only very few and small necroses could be detected. In contrast, the much smaller, growth-inhibited tumour cell implants had an onion-like histological appearance, which was characterized by different tissue layers: a large, central necrosis was surrounded by a dense layer of viable tumour cells (Fig. 3*c*, *e*). Invasion of this tumour had not progressed, as evidenced by the presence of natural structures of the skin, such as the muscular cell layer (Fig. 3*f*).

The distribution of capillaries and blood vessels in the tissue specimens was determined by incubating frozen tissue sections with a rat monoclonal antibody specific for the endothelial cell adhesion antigen PECAM[14]. The tumours co-implanted with the control virus-producing cells displayed the pattern of capillaries and vessels expected for well-vascularized tissue (Fig. 4*a*), whereas the growth-inhibited tumour cell implant showed a large central tumour cell necrosis, which was surrounded by a layer of viable tumour cells lacking blood vessels or capillaries (Fig. 4*b*). The tumour cells in this layer showed a higher cell density than the control tumour, suggestive of a reduction in tumour-induced oedema. As VEGF seems to induce vascular permeability *in vivo*, and is also designated vascular permeability factor, inhibition of VEGF/Flk-1 interaction may inhibit tumour-associated oedema.

Flk-1 expression in the proliferating endothelial cells of the tumour was confirmed by *in situ* hybridization of tissue sections with a ^{35}S-labelled Flk-1-specific antisense complementary DNA probe[7]: distribution was the same as immunostaining with endothelial cell-specific antibodies, indicating that proliferating endothelial cells expressed Flk-1 (Fig. 4*c*). *In situ* hybridization with a neomycin-resistance gene (*neo*^{r}) antisense probe confirmed the presence of retroviral sequences. As shown in Fig. 4*d*, the entire Flk-1 dominant-negative-inhibited tumour, consisting of the retrovirus-producing and infected cells, was *neo*^{r}-positive, which matched the result obtained with a Flk-1-specific probe (not shown). The morphology of tumours that had been co-implanted with control virus-producing cells was very similar, but the virus-producing cells were extensively infiltrated by infected tumour cells. In these tumours, which contained many capillaries and blood vessels, *neo*^{r}-positive signals were also found in endothelial cells (not shown).

Experiments with other tumour types (not shown) support these results from the C6 glioblastoma model and indicate that solid tumour growth can be inhibited by prevention of angiogenesis, a process normally regulated by VEGF, which when secreted by tumour cells attracts and stimulates Flk-1-positive vascular endothelial cells in a paracrine fashion.

The ability to block VEGF-mediated signal transduction with the Flk-1 dominant-negative mutant emphasizes the central role of the Flk-1/VEGF system in tumour angiogenesis and further supports the contention that this system is the major regulator of angiogenesis and vasculogenesis in the whole organism. Our results are consistent with the observation that neutralizing antibodies against VEGF suppress tumour growth *in vivo*[15], and suggest that the function of the alternative VEGF receptor, Flt-1 (ref. 16), is either not relevant in this system or may be blocked by heterodimer formation with the Flk-1 TM mutant. Moreover, with the identification of Flk-1 as a regulator molecule that is specific and crucially important for solid tumour progression, a variety of strategies for the development of clinical applications can be considered. For glioblastoma, a tumour with generally poor prognosis and resistance to all available therapies, retrovirus-mediated gene therapy may be advantageous, because non-mitotic brain tissues such as neurons, glia and quiescent endothelial cells would not be infected. In fact, preliminary experiments revealed that even treatment of established C6 glioblastoma tumours with Flk-1 TM retrovirus particles significantly inhibited tumour progression (Fig. 2*b*). Although further investigation will be necessary to develop this laboratory model into a clinically applicable gene therapy, the Flk-1 receptor system is a promising target for the development of specific anti-tumour drugs. □

Received 20 September; accepted 21 December 1993.

1. Folkman, J. *J. natn Cancer Inst.* **82,** 4–6 (1990).
2. Folkman, J., Watson, K., Ingber, D. & Hanahan, D. *Nature* **339,** 58–61 (1989).
3. Risau, W. *Progr. Growth Factor Res.* **2,** 71–79 (1990).
4. Folkman, J. & Klagsbrun, M. *Science* **235,** 442–447 (1987).

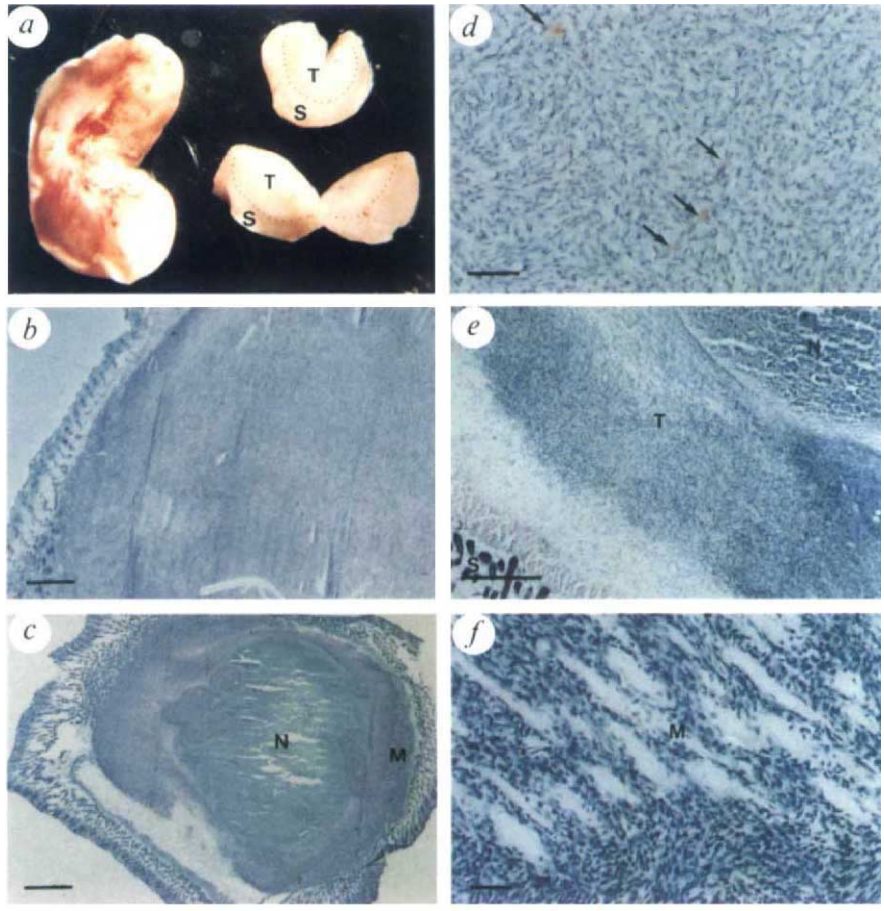

FIG. 3 Features of Flk-1 dominant-negative-inhibited tumours. *a*, Resected specimen: control tumours are on the left, an inhibited tumour is on the right. Black dots indicate the borderline between implanted cell-derived (T) and surrounding normal skin tissue (S). *b*, Frozen section of control tumour stained with toluidine blue (low magnification), showing viable tumour cell mass without visible necroses. *d*, Haematoxylin/eosin-stained section of the same tumour at higher magnification. Red staining (arrows) indicates the presence of blood vessels. *c*, Toluidine blue, and *e*, *f*, haematoxylin/eosin-stained sections of the Flk-1 dominant-negative inhibited cell implant. A large central necrosis (N) surrounded by a layer of viable tumour cells and the muscular layer (M) of the skin is visible. Morphometric examination of the tumours revealed necrotic areas of 3% in the control tumour and 27% in the inhibited tumour cell implant. These features were evident in several tumours of all groups.
METHODS. Tumour specimens were embedded in tissue-tek (Miles) and frozen in liquid nitrogen. 10-μm-thick sections were cut with a cryostat (Leica) and stained histologically with toluidine blue or haematoxylin/eosin. Bar represents 1 mm (*b*, *c*) or 400 μm (*d*, *e*, *f*).

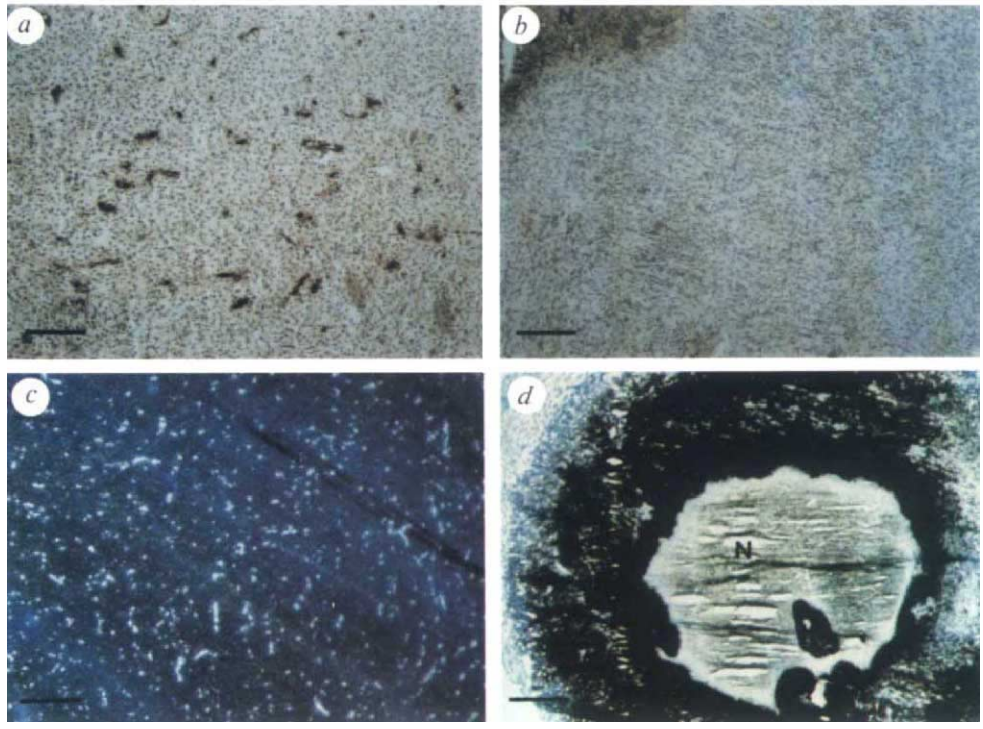

FIG. 4 *In situ* hybridization and immunohistochemical staining of tissue sections. Sections of control tumour (*a*) and Flk-1 dominant-negative inhibited tumour (*b*) immunohistochemically stained with a rat monoclonal antibody against the endothelial antigen PECAM. *c*, *In situ* hybridization of the control tumour with Flk-1 specific ^{35}S-labelled antisense probe; darkfield illumination. *d*, Brightfield illumination of an *in situ* hybridization with a *neo*^{r}-specific antisense probe of the angiogenesis-inhibited tumour. The central necrosis of the tumour is surrounded by tissue with high expression of *neo*^{r} and consisting of the virus-producing and infected cells.
METHODS. Immunohistochemistry and *in situ* hybidization on frozen sections has been described[7]. Signals were the same, but weaker, with antibodies against von Willebrand factor. For *in situ* hybridization, Flk-1 antisense cDNA comprising the 5′-2,619 bp of the receptor cDNA or an antisense cDNA of the *neo*^{r} gene, respectively, were used as probes. Autoradiogram exposure was three days. There was no specific hybridization with the sense probes. N, necrosis. Bar represents 400 μm (*a*–*c*) or 1 mm (*d*).

5. Plate, K. H., Breier, G., Weich, H. A. & Risau, W. *Nature* **359,** 845–848 (1992).
6. Shweiki, D., Itin, A., Soffer, D. & Keshet, E. *Nature* **359,** 843–848 (1992).
7. Millauer, B. *et al. Cell* **72,** 835–846 (1993).
8. Plate, K. H., Breier, G., Millauer, B., Ullrich, A. & Risau, W. *Cancer Res.* **53,** 5822–5827 (1993).
9. Kashles, O., Yarden, Y., Fischer, R., Ullrich, A. & Schlessinger, J. *Molec. cell. Biol.* **11,** 1454–1463 (1991).
10. Redemann, N., Holzmann, B., Wagner, E. F., Schlessinger, J. & Ullrich, A. *Molec. cell. Biol.* **12,** 491–498 (1992).
11. Amaya, E., Musci, T. J. & Kirschner, M. W. *Cell* **66,** 257–270 (1991).
12. Ueno, H., Colber, L. H., Escobedo, J. A. & Williams, L. T. *Science* **252,** 844–848 (1991).
13. Miller, A. D. & Rosman, G. J. *Biotechniques* **7,** 980–988 (1989).
14. Newman, P. J. *et al. Science* **247,** 1219–1222 (1990).
15. Kim, K. J. *et al. Nature* **362,** 841–844 (1993).
16. De Vries, C. *et al. Science* **255,** 989–991 (1992).
17. Chen, C. & Okayama, H. *Molec. cell. Biol.* **7,** 2745–2752 (1987).
18. Gorman, C. M., Gies, D., McCray, G. & Huang, M. *Virology* **171,** 377–385 (1989).
19. Stewart, C. L., Schuetze, S., Vanek, S. & Wagner, E. *EMBO J.* **6,** 383–388 (1987).

ACKNOWLEDGEMENTS. We thank M. Longhi and L. Taylorson for assistance in tumour implantation experiments, E. Dejana for the anti-PECAM antibody, M. Clauss for ^{125}I-VEGF, and J. Arch for preparing the manuscript.